Thermochimica Acta, 68 (1983) 165–186
Elsevier Science Publishers B.V., Amsterdam – Printed in The Netherlands

EFFECTS OF PRESSURE ON BIOMASS PYROLYSIS. II. HEATS OF REACTION OF CELLULOSE PYROLYSIS

WILLIAM S.-L. MOK and MICHAEL J. ANTAL, Jr. *

Department of Mechanical and Aerospace Engineering, Princeton University, Princeton, NJ 08544 (U.S.A.)

(Received 23 March 1983)

ABSTRACT

A Setaram DSC in conjunction with stainless steel pressure vessels was used to investigate the effects of pressure and purge gas flow rate (gas phase residence time) on the heat demands of cellulose pyrolysis. High pressure and low flow rate reduce the heat of pyrolysis and increase char formation. Experiments were conducted to investigate the pyrolysis reactions of anhydrocellulose and levoglucosan, the two major intermediate products in cellulose pyrolysis. Separate models for the degradation of each intermediate were postulated and combined to form a detailed mechanistic model for cellulose pyrolysis. The model explains all the observed effects of pressure and flow rate.

INTRODUCTION

Understanding the effects of pressure on biomass pyrolysis is of particular importance in the design of gasifiers and pyrolysis reactors. Unfortunately, little experimental data are available. An earlier paper [1] described experimental studies of the effects of pressure and small quantities of oxygen on the product distribution of cellulose pyrolysis. In this paper, the effects of pressure on the heats of reaction of cellulose pyrolysis will be discussed.

To explain the observed effects, the pyrolysis mechanism must first be studied. The generally accepted mechanism for cellulose pyrolysis based on

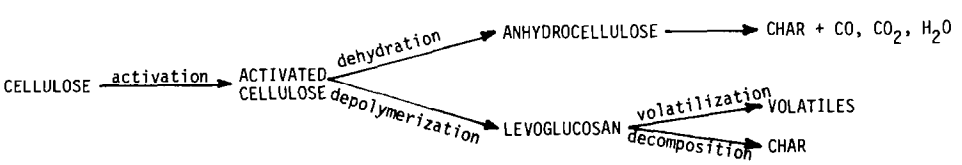

Fig. 1. Mechanism for cellulose pyrolysis prior to the present work.

* Present address: University of Hawaii, Hawaii Natural Energy Institute, Honolulu, HI 96822, U.S.A.

0040-6031/83/$03.00

the work of Kilzer and Broido [2], Arseneau [3], and Bradbury et al. [4] (Fig. 1) features two major solid phase reactions competing for the activated cellulose, leading to the formation of anhydrocellulose by the dehydration route and levoglucosan by depolymerization. The anhydrocellulose eventually forms char and permanent gases; while levoglucosan can further decompose to form other volatiles and gases. However, the details of these secondary reactions are not well understood. This paper also discusses two branch series of experiments conducted to investigate the secondary reactions. Separate models are proposed to describe the further pyrolysis reactions of anhydrocellulose and levoglucosan, and then combined to form a detailed mechanism for cellulose pyrolysis. This mechanism explains all the observed effects of pressure and flow rate on the char yields and heats of reaction of cellulose pyrolysis.

EXPERIMENTAL

Apparatus

As indicated in Fig. 2, the apparatus consisted of two stainless steel reactors embedded in a differential scanning calorimeter, together with appropriate flow control devices.

Differential scanning calorimeter

The Setaram (France) differential calorimeter (DSC) is unique because of its tubular design. This design allows one to measure the heat of reaction of a process as it occurs inside a flow reactor. Two identical ceramic reactor tubes are symmetrically located inside a furnace, which is capable of raising the temperature of the reactors from subambient to 827°C at rates up to 20°C min^{-1}. At any moment, a constant temperature is kept along the length of the reactor to prevent lateral heat loss. Hundreds of opposed

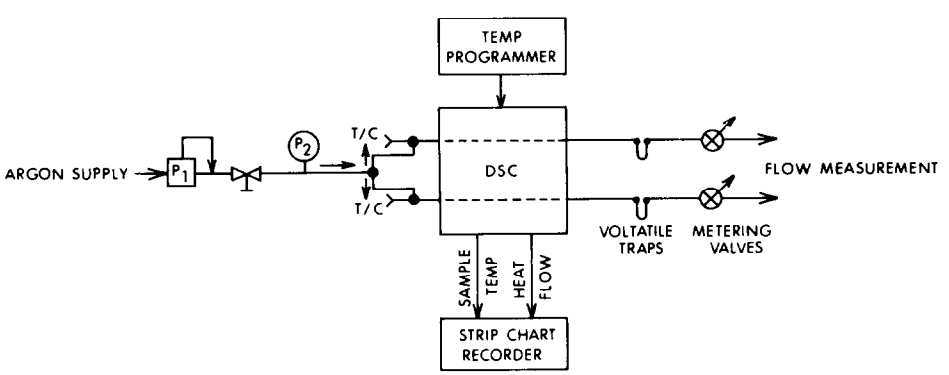

Fig. 2. Apparatus schematic.

thermocouples are strategically located along the reactor tubes, each designed to measure the temperature difference across two points along a radius. With known thermoproperties between the two thermocouple junctions, this temperature difference translates into a radial heat flow. Temperature differences along the many radii along the length of the sample tube are summed, and subtracted from the corresponding sum along the reference tube to give one differential heat flow signal between the sample and the reference reactor. The integration of this signal over time gives the heat of reaction for any chemical or physical process occurring within the sample tube.

Micro tubular reactors

The two micro reactors, with an internal diameter of 4.64 mm, were fabricated from type 316 stainless steel. They were designed to: (1) provide reactor communication with the DSC sensor, (2) minimize lateral heat flow along the tube by varying reactor wall thickness, and (3) allow repeated operations at 25 atm and 800°C.

Purge gas flow

A tank of argon with a pressure regulator was used to control the total pressure of the reactors. Nupro fine metering valves (SS-2SGD) at the reactor exits allowed precise flow control. Two 8- in. columns of GC packing material (Altech Molecular Seive 5a) were installed before the exit valves to stop volatile materials from entering the valves and altering the flow during pyrolysis. Among the various inert gases, argon was used because with a fixed valve flow coefficient, its higher density permits precise flow control at a lower volumetric flow rate.

Samples

Whatman No. 1 filter paper (0.06% ash), cut into rectangular strips (10 mm × 2 mm) was used as the cellulose feedstock. Levoglucosan was synthesized by destructive distillation of cornstarch [5].

Procedures

The pressure regulator and exit valves were first adjusted to achieve the desired pressure and flow rate. A weighed sample was then inserted into the micro reactor using a specially designed steel sample boat containing a type K thermocouple positioned to be in direct contact with the sample. The DSC then raised the temperature of the reactor from 27°C to 500°C at 5°C min^{-1}. The heat flow signal and the sample temperature were recorded by a Linear Model 385 two-pen strip chart recorder. The system was then depressurized and the sample boat removed. The residue was collected and

weighed. The area under the peak on the thermogram was determined by cutting and weighing.

During the first few experiments, the sample was not immediately removed after the sample run. Instead, the reactors were cooled to 27°C. The charred sample was then reheated following the earlier temperature history in order to obtain a base line, or more accurately, a thermogram of the char for reference. Flat base lines around the pyrolysis temperature were consistently observed. Consequently, straight lines across the base of the peak were used for area determination.

For subatmospheric experiments, the reactors were flushed with argon after sample insertion. A mechanical vacuum pump was then attached to the reactor exits to generate a vacuum. No accurate provision was made to control the flow rate. Instead, to simulate a high flow, the vacuum pump was kept on throughout the experiment. When a 'low' flow was desired, the pump was turned off after evacuation, so that no external force would be available to sweep away the volatiles.

DSC calibration

Indium, tin, lead and zinc were used as heat of fusion standards to calibrate the sensitivity of the DSC in the temperature range 150–420°C. Experiments with each metal were carried out at various pressures and flow rates of purge gas. Depending on the heat of fusion of each metal, samples weighing between 15 and 40 mg were used. The calibrant was heated at 5°C min^{-1} from ambient to 30°C below the melting point. After the system stabilized, it was heated again at 5°C min^{-1} to 30°C above the melting point. The peak obtained (a typical one is shown in Fig. 3) was then analyzed to determine the calibration coefficient.

Good reproducibility of the data was obtained. Variance in the measurements of the sensitivity coefficient calibration under different pressure, flow

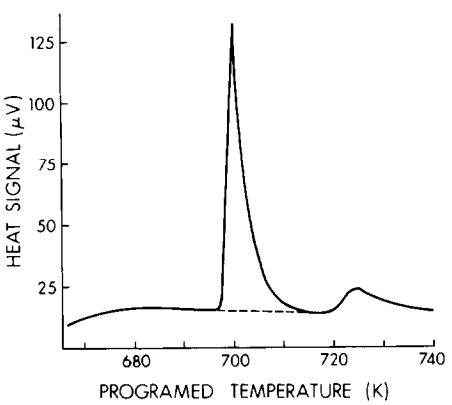

Fig. 3. DSC peak from a calibration experiment (8 mg of zinc was heated at 1 atm with 3 cc min^{-1} flow of argon).

TABLE 1

List of calibrants used in the determination of the DSC sensitivity coefficient

Calibrant	Source	M.p. (°C)	Lit. range of ΔH_{fusion} (J g^{-1})	ΔH_{fusion} used (J g^{-1})	Calibrant coefficient (μV mW^{-1})
Indium	NPL, London CRM NO M16-01	156.6	28.377–28.458	28.33 NPL certified	6.09 ± 0.1
Tin	NBS SRM NO 42g	232	56.167–60.709	60.683 Metals handbook	6.37 ± 0.3
Lead	NBS SRM NO 49e	327.5	23.162–26.284	23.2287 NBS verbal	6.74 ± 0.2
Zinc	Dupont DSC Calibrant	419.5	100.817–113.204	113.204 Dupont specified	6.53 ± 0.3

rate and sample mass amounted to less than 3%. Temperatures measured by the thermocouple in direct contact with the sample agreed to within 1°C. However, such precision did not imply that the measured sensitivity was accurate to within 3%. Of all the metals used, only indium had a certified heat of fusion. The remaining heats of fusion were taken from literature data. A comparison of the literature revealed significant differences in the reported heats of fusion. Consider for example the calibration using a lead standard. Depending on the source of heat of fusion data, the sensitivity could range from 6.53 to 7.34 μV mW^{-1}, amounting to more than 12% error in subsequent measurements of ΔH. Table 1 summarizes the series of standards used, together with the range of reported heats of fusion.

In Fig. 4, the sensitivity of the DSC was plotted against temperatures, while the original DSC calibration curve was included for comparison.

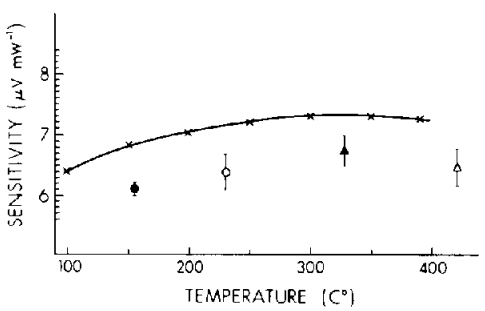

Fig. 4. Plot of DSC sensitivity vs. temperature. Calibration based on the heat of fusion of indium(●), tin(○), lead (▲) and zinc (△). The original Setaram calibration curve (×) is included for comparison.

Calibration based on lead was used in the analysis of experimental results because its melting point falls closest to the cellulose pyrolysis temperature.

Choice of experiments

Experiments were conducted at pressures of 10^{-2}, 1, 2, 5, 10 and 25 atm. A series of test runs at atmospheric pressure showed that the results were also very sensitive to the volumetric flow rate of purge gas through the reactors, but the effects seemed to asymptote at 20 cc min^{-1}. Consequently, three different flow rates were used at each pressure. At 1 atm, argon flows of 1, 5 and 20 cc min^{-1} were used. The ideal gas continuity relationship was used to calculate the suitable flows for the high pressure experiments, such that the same flow velocities, hence residence times, were maintained. For example, flows of 10, 50 and 200 cc min^{-1} of argon (measured after the exit valves at atmospheric pressure) were actually used for the 10 atm pressure experiments. For the rest of the discussion, the three 'normalized' volumetric flows of 1, 5 and 20 cc min^{-1} will be referred to as low, medium and high flows. Subatmospheric experiments were run with both "low" and "high" flows, manipulated by the operation of the vacuum pump.

RESULTS AND DISCUSSION

Very similar thermograms were observed for all of the experiments. Each showed only 1 peak with a fairly symmetrical shape, starting at around 330°C, peaking at 370°C and ending near 390°C. This peak is a representation of the overall heat effect of the entire pyrolysis process, and is not resolved to indicate individual pyrolysis reactions as were observed by some earlier workers [2,6]. Some typical thermograms can be seen in Fig. 5.

Results of this series of experiments (see Figs. 6–9) show that with increasing pressure and decreasing flow rate, the heat of pyrolysis, ΔH_{pyr}, decreases, while the char yield increases. The char yields from low flow experiments scatter considerably more than the yields from high flow

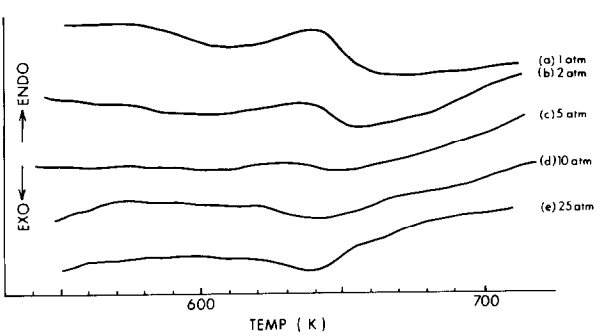

Fig. 5. Thermograms for cellulose pyrolysis under a low flow.

experiments. While the increase in ΔH_{pyr} from 1 atm pressure to vacuum is particularly dramatic, there is no corresponding decrease in the char yields.

Before these observations can be explained, the branch series of experi-

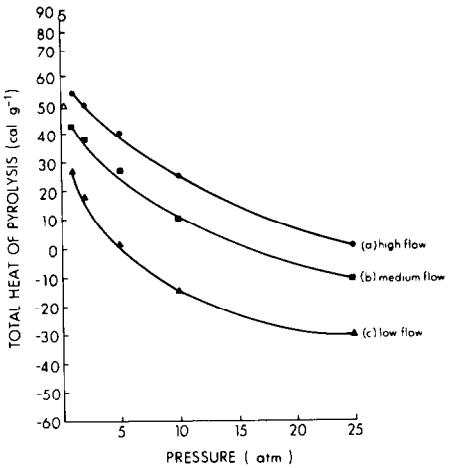

Fig. 6. Plot of total heat of cellulose pyrolysis vs. pressure for various flows of purge gas, or high(●) and low(▲) rates of volatile removal under vacuum.

ments conducted to investigate the details of the cellulose pyrolysis mechanism must first be discussed.

Secondary reactions of anhydrocellulose

It is known that at low temperatures the dehydration of cellulose to anhydrocellulose occurs to a greater extent than depolymerization to levoglu-

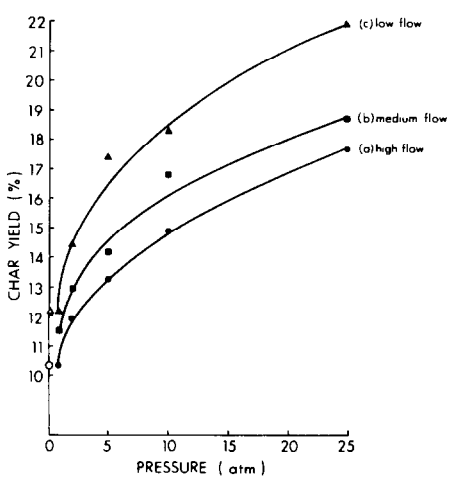

Fig. 7. Plot of char yields vs. total pressure for various flows of purge gas, or high(●) and low(▲) rates of volatile removal under vacuum.

cosan [2,4]. To study the effects of pressure on the further reactions of the anhydrocellulose, experiments involving sustained preheating of the cellulose substrate were conducted. In this series of experiments, the cellulose sample

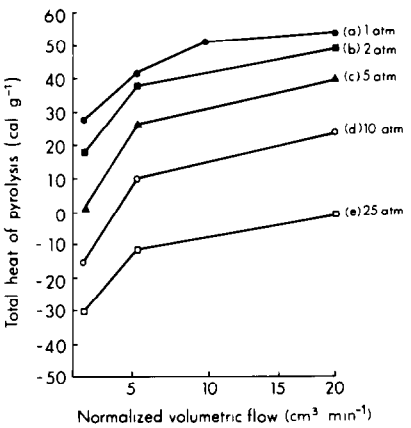

Fig. 8. Plot of total heat of cellulose pyrolysis vs. normalized volumetric flow of purge gas.

was heated at 5°C min^{-1} from 27 to 240°C, and held for 2 h before continuing the normal pyrolysis temperature history. For one experiment, the preheating was held at 270°C for 2.5 h. Experiments were conducted at 1 and 10 atm pressure, with both low and high flows. The results appear in Table 2.

Calculations based on the rate data of Bradbury et al. [4] showed that approximately 3% of the cellulose would have reacted and become anhydrocellulose after preheating at 240°C for 2 h, and 18% after 2.5 h at 270°C. On

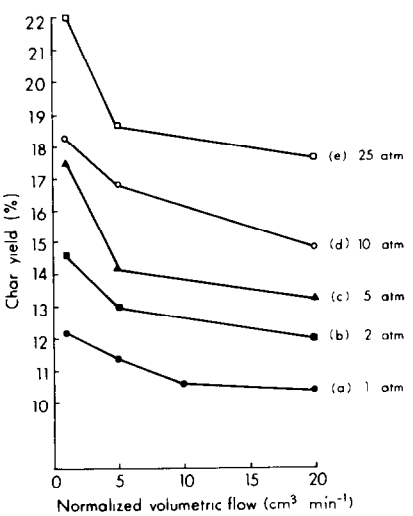

Fig. 9. Plot of char yields vs. normalized flow of purge gas.

TABLE 2

Results of cellulose pyrolysis experiments with preheating treatment

Experiment	Preheating temp. (°C)/time (h)	Flow	Pressure (atm)	ΔH_{pyr}(cal g^{-1})	Char(%)
a	240/2	Low	1	−16	15
b	240/2	Low	10	−34	21
c	240/2	High	1	53	11
d	240/2	High	10	17	15.5
e	270/2.5	High	1	48	12

the other hand, it was estimated that approximately 30% of the cellulose degrades via anhydrocellulose under the normal experimental conditions. Therefore, preheating provides a significant amount of additional anhydrocellulose (3% by weight of cellulose, but 10% of the total anhydrocellulose that would subsequently form), without significantly altering the rest of the pyrolysis chemistry (since 95% remained as cellulose). Consequently, the difference between experimental results with and without preheating should be indicative of the pyrolysis chemistry of the additional anhydrocellulose.

The differences between results of pyrolysis with and without preheating are shown in Table 3. This Table shows that preheating produces a higher char yield and a lower heat of pyrolysis. In particular, a comparison of the results of experiments c and e shows that the char yield increases and the heat of pyrolysis decreases with an increase in preheating time and temperature. These results confirm literature findings that at low temperature, cellulose dehydration leading to char formation plays an increasingly important role in the pyrolysis process. What is more interesting is that the effect of preheating is far more dramatic with a low flow (experiments a and b), where the heat of pyrolysis actually turns from endothermic to exothermic (see Table 2).

Literature results [2] show that the predominant products of further

TABLE 3

The effects of preheating in cellulose pyrolysis

Experiment	Preheating temp. (°C)/time (h)	Flow	Pressure (atm)	$\Delta(\Delta H_{pyr})$ [a] (cal g^{-1})	ΔChar (%) [b]
a	240/2	Low	1	−43	2.5
b	240/2	Low	10	−19	2.5
c	240/2	High	1	−1	0.5
d	240/2	High	10	−8	0.5
e	270/2.5	High	1	−6	1.5

[a] ΔH_{pyr}(with preheat) − ΔH_{pyr}(standard procedure).

[b] Char(with preheat) − Char(standard procedure).

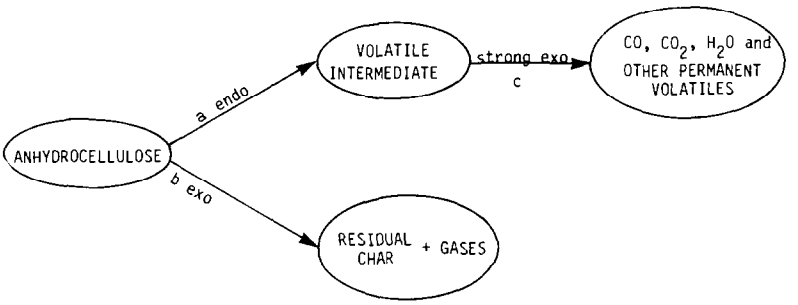

Fig. 10. Proposed mechanism for anhydrocellulose pyrolysis.

anhydrocellulose reactions include char and permanent gases, and that formation of gases such as CO, CO_2 and H_2O is strongly exothermic. Kilzer and Broido [2] have suggested that other volatile products, such as acetaldehyde and formaldehyde, also form exothermically due to the formation of C=O double bond. Roberts [7], in his discussion of the results of Lipska and Parker [8], proposed that volatiles form from a nonvolatile intermediate. This intermediate could presumably be anhydrocellulose.

Taking these findings into consideration, a proposed model which describes the pyrolysis reactions of anhydrocellulose is depicted in Fig. 10. This model features a pair of competitive reactions which lead immediately to a reactive volatile intermediate in one case, and char plus gases in the other. The volatile intermediate undergoes further pyrolysis to form CO, CO_2, H_2O and other gases. The postulate of a volatile intermediate is necessary to explain why a high flow significantly diminishes the effect of preheating on ΔH_{pyr}. With a high flow, the newly formed volatile intermediates are swept away from the DSC sensor, so that subsequent vapor phase reactions, which contribute the major exothermic effect (reaction c), are either quenched or simply not seen by the DSC. In the literature, char formation reactions are thought to be exothermic [2]. The present results, as will be discussed shortly, support this conclusion. On the other hand, experiment c (Table 3) indicates an approximately autothermic result, suggesting a balanced heat effect between reactions a and b (Fig. 10). Since reaction b (char formation) is exothermic, reaction a must thus be endothermic.

The reasons for choosing this model should be stressed: (1) it explains all experimentally observed behavior of anhydrocellulose, (2) it is in agreement with existing literature concerning anhydrocellulose, and (3) it features the same type of competitive reactions found in the degradation scheme of cellulose and levoglucosan, which, as discussed in ref. 9, is consistent with the 'competitive' mechanistic framework governing the pyrolysis of many organic compounds.

The proposed mechanism can now be used to explain the data shown in Table 3. Since these data are being interpreted as results of pyrolysis of the

TABLE 4

Estimated [a] ΔH_{pyr} and char yields from pyrolysis of anhydrocellulose

Experiment	Starting amount of anhydrocellulose (% of cellulose)	Flow	Pressure (atm)	ΔH_{pyr} (cal g^{-1})	Char (%)
a	3	Low	1	−1433	83
b	3	Low	10	−633	83
c	3	High	1	−33	17
d	3	High	10	−270	17
e	18	High	1	−33	8

[a] These numbers are derived from the difference data of Table 3 normalized by the small percentage of initial anhydrocellulose.

additional anhydrocellulose, it is more instructive to discuss it on a per weight of anhydrocellulose basis. Therefore, the data of Table 3 are normalized by the weight of initial anhydrocellulose (estimated to be 3% of cellulose in experiments a–d, 18% in experiment e), and presented in Table 4.

Under a high flow situation, reaction c (Fig. 10) can be ignored. At 1 atm pressure, the competitive reactions a and b split in such a way as to bring about a combined heat effect of −33 cal g^{-1} (of anhydrocellulose). Although Table 4 indicates no significant char difference due to pressure, the increase in exothermicity at 10 atm leads to the conclusion that pressure favors reaction b (exothermic char formation). Since the char yields of Table 4 are based on the difference between two cellulose pyrolysis experiments, both evidencing a considerable amount of scatter, it is likely that any small effects caused by pressure are buried amidst the variance in the original data. Note that after normalization, the heats of pyrolysis from experiments c and e agree with each other. This furnishes strong support for the assumption that the difference reflects anhydrocellulose reactions, and also the validity of the normalization procedure.

The low flow studies include reaction c, which is strongly exothermic. The heat generated by this reaction lowers the observed overall heat of reaction to −1433 cal g^{-1} at 1 atm pressure. Pressure still favors exothermic reaction b, but route a now brings in additional exothermicity from reaction c. The combination of routes a and c liberates more heat than route b. Therefore, at 10 atm pressure, the overall heat of reaction of anhydrocellulose pyrolysis is less exothermic.

To summarize, the ΔH_{pyr} data for anhydrocellulose are furnished by the differences between results of cellulose pyrolysis with and without preheating. The validity of this procedure is supported by the consistency of data obtained from experiments generating different amounts of additional anhydrocellulose. A simple mechanism for the decomposition has been postulated. This mechanism adequately explains the observed data, and how

exothermicity is increased by pressure in one case, but decreased in the other.

Secondary reactions of levoglucosan

The second major reaction in cellulose pyrolysis involves depolymerization, leading immediately to the formation of levoglucosan. Four experiments using levoglucosan as the sample, at 1 and 10 atm with both low and high flows, were conducted to investigate the further pyrolysis reactions of this intermediate product.

The thermograms, shown in Figs. 11 and 12, indicate the very complex thermal behaviors of levoglucosan pyrolysis. In all four cases, the first major endothermic peak occurs at 117°C, during the solid phase transition of levoglucosan into a plastic crystal state [10]. This is followed by a smaller endothermic peak at the melting point (175°C). At higher temperatures, the thermal response varies according to the pressure and flow rate.

On the 1 atm high flow thermogram (Fig. 11a), the start of a major endotherm near 220°C indicates the onset of boiling. A transition occurring near 290°C interrupts the endothermic rise, the abruptness of which indicates a sudden exothermic heat release. However, another endothermic reaction takes over near 310°C, and gives rise to an endothermic peak near 330°C. At 10 atm pressure (Fig. 11b), still under a high flow, the boiling point is raised considerably to 260°C. A sharp exothermic swing occurs at the temperature corresponding to the abrupt transition on the 1 atm thermogram. This time, the exotherm is interrupted by concurrent endothermicities at 300°C. The dominant exotherm ends near 360°C.

Under low flow conditions (Fig. 12), no boiling phenomenon can be seen. At 1 atm pressure, the complex thermogram can be best interpreted as one large exotherm, spanning temperatures from 280°C to 360°C. Superimposed

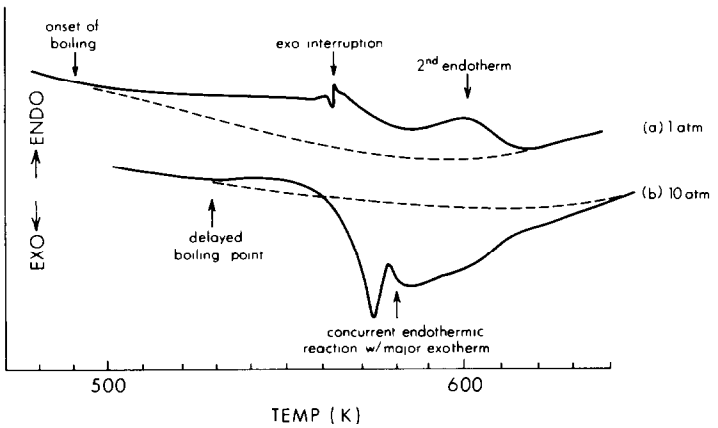

Fig. 11. Thermograms for levoglucosan pyrolysis under a high flow.

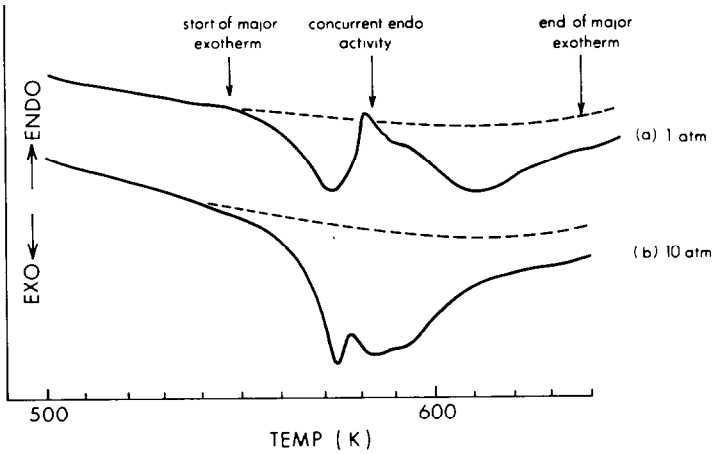

Fig. 12. Thermograms for levoglucosan pyrolysis under a low flow.

on this exotherm is an endotherm from 300°C to 340°C. A similar interpretation can be made for the 10 atm case, although the exothermicity is much sharper and more dominant, and the interrupting endothermicity relatively less significant.

Putting all four thermograms together, we can conclude that there are three main heat effects: (1) endothermic evaporation starting at 220°C at 1 atm, but at a considerably higher temperature at 10 atm, (2) a major exothermic reaction occurring from around 280–360°C, and (3) a smaller but significant endothermic reaction taking place from 300–340°C, concurrent with the major exothermic reaction. The relative dominance of each of these three reactions varies according to the experimental conditions.

The information provided by these DSC studies, together with others furnished by TGA, DTG and Friedman curves obtained earlier in this laboratory [11] offer some insights into the levoglucosan pyrolysis mechanism. The research of Arseneau [3] and Broido et al. [12] suggested two major effects of heat on levoglucosan: evaporation or thermal decomposition. If the physical environment facilitates the escape of volatiles, levoglucosan vaporizes; whereas under mass transfer limiting conditions, levoglucosan undergoes exothermic decomposition to form char. In our experiment, low flows and high pressures represent conditions which inhibit the escape of levoglucosan. Table 5 shows that char yields are much higher at high pressures. At low pressures, the small quantities of char were found scattered all over the sample cup, indicating large movements caused by evaporation. High pressure and low flow thus favor the char forming route among the two competitive reactions.

Under a high flow at 1 atm, an initial domination by evaporation is evident. By 290°C, decomposition becomes more significant, as suggested by the abrupt transition of Fig. 11a. But since much of the levoglucosan has

TABLE 5

Char yields from pyrolysis of levoglucosan (%)

Pressure (atm)	Flow	
	Low	High
1	8	$1\frac{1}{2}$
10	23	20

already vaporized, the heat released by the decomposition of the remaining levoglucosan is not sufficient to generate an exotherm. In contrast, at 10 atm, levoglucosan did not begin to vaporize until shortly before the decomposition reaction. As a result, most of the material is decomposed, as evidenced by an overall exotherm.

Under low flow conditions, evaporation is inhibited. Consequently, the corresponding endotherm is absent. The low flow thermograms are clouded by secondary vapor phase reactions. However, it can be argued that the relative steepness of the exothermic drop at 10 atm supports the conclusion that exothermic decomposition is favored at high pressure.

The hypothesis of two competitive reactions is further supported by Friedman curves (Fig. 13) derived from TGA data. Friedman curves are plots of activation energies against percentage of conversion. Each activation energy at a particular level of conversion is obtained by applying the Friedman analysis [13] to a set of weight loss curves over many heating rates. The curves (Fig. 13) show initially a noisy but relatively constant low value of the apparent activation energy, which is indicative of a boiling phenomenon. The downward tail is known to be a unique signature [14] of a pair of competitive reactions, with a higher activation step leading to more char.

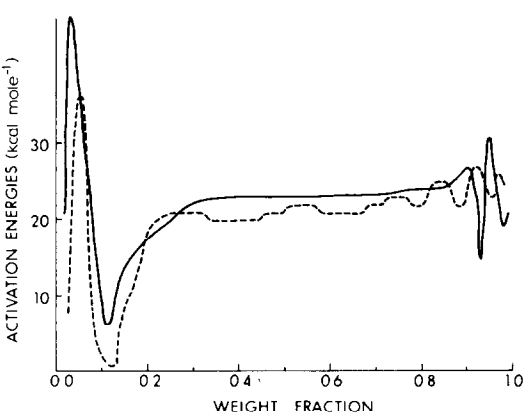

Fig. 13. Friedman curves of pyrolysis of levoglucosan. ------, Low heating rates; ———, high heating rates.

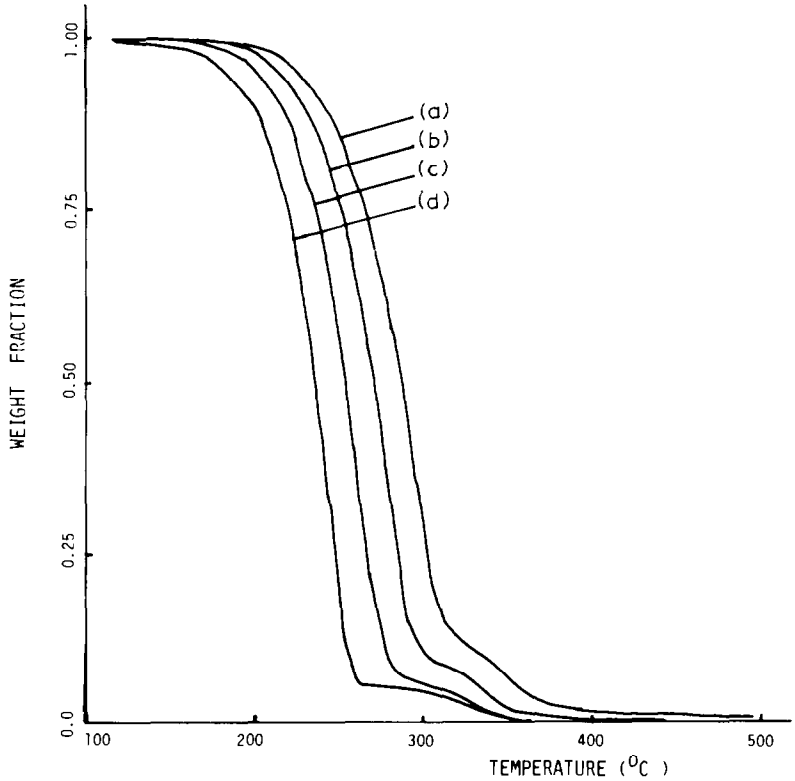

Fig. 14. Thermogravimetric curves for levoglucosan pyrolysis at heating rates of (a) 21°C min^{-1}, (b) 11°C min^{-1}, (c) 5°C min^{-1} and (d) 2°C min^{-1}.

This agrees with the suggested scheme of competitive reactions for levoglucosan, since evaporation (boiling) is characterized by an apparent low E (reflecting the low temperature sensitivity of a heat transfer limiting condition), and leads to no char.

Of the three major heat effects mentioned earlier, two have been accounted for. The endotherm is indicative of evaporation. The major exotherm is caused by decomposition of levoglucosan. Antal [15] has obtained evidence that levoglucosan undergoes further competitive pyrolytic reactions in the vapor phase, leading to a refractory tar in one case, and permanent gases in the other.

The third heat effect, i.e. the interrupting endotherm concurrent (in most cases) with the major exotherm, remains to be explained. Thermogravimetric curves (Fig. 14) show abrupt transitions approaching the end of conversion, indicating a different mechanism controlling the final weight loss. Derivative (DTG) curves (Fig. 15) point to this reaction as a second peak, occurring at the same temperature as the 'interrupting' endotherm observed in the DSC data. Since this reaction is detectable by the TGA, it must be a solid phase

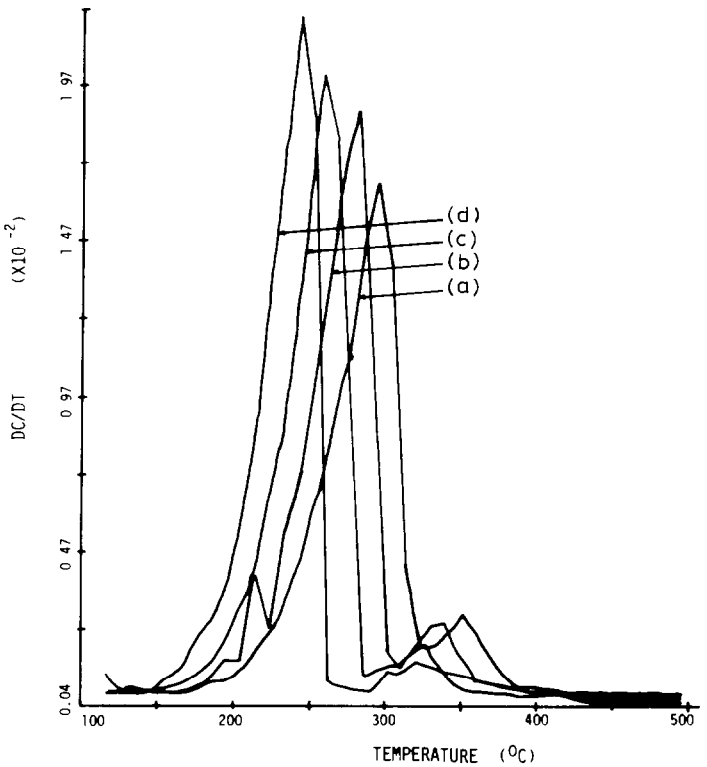

Fig. 15. DTG curves for levoglucosan pyrolysis at heating rates of (a) 21°C min^{-1}, (b) 11°C min^{-1}, (c) 5°C min^{-1} and (d) 2°C min^{-1}.

reaction. Its occurrence towards the very last part of the weight loss suggests that it is a reaction of the residues formed by the earlier major competitive reactions. The observation that the transition to this reaction occurs earlier (higher weight fraction) with a higher heating rate supports this suggestion. With a higher heating rate, more time is spent in the temperature regime where decomposition dominates, leading to a larger weight fraction of residue. Consequently, residual reactions occur at a higher weight fraction. The part of the Friedman curve relevant to this residue reaction shows an extraordinary upswing in activation energy. This upswing is a signature of competitive reactions, with the higher activation energy process leading to less char formation. The DTG peaks relevant to this residual reaction show a rise in peak height with increasing heating rate, which is another signature [16] of competitive reactions.

The above discussion of levoglucosan pyrolysis can be summarized by the mechanistic model depicted in Fig. 16. Initially, two reactions compete for the levoglucosan: evaporation, or decomposition to form a residue. High pressure, low flow of purge gas, and high heating rates favor the decomposition route. Levoglucosan vapor undergoes further competitive reactions

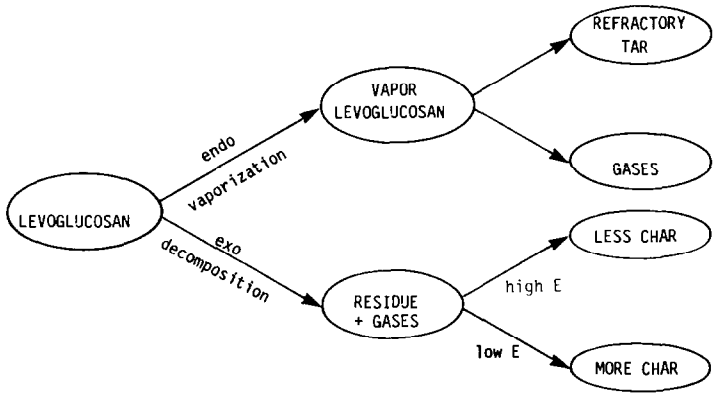

Fig. 16. Mechanism for levoglucosan pyrolysis.

leading to a refractory tar or gases. Residue from the levoglucosan decomposition path undergoes further pyrolysis by another set of competitive reactions. The mechanism of levoglucosan polymerization leading to a higher molecular weight residue is well known in the literature [17].

Discussion of cellulose pyrolysis

Combining the above new findings with the existing knowledge, a more detailed mechanism for cellulose pyrolysis (Fig. 17) can be postulated. Effects of pressure and flow rate can now be explained in terms of this mechanism.

The major reason for the increased ΔH_{pyr} under a high flow is due to the rapid removal of the evolving volatile intermediates and quenching of

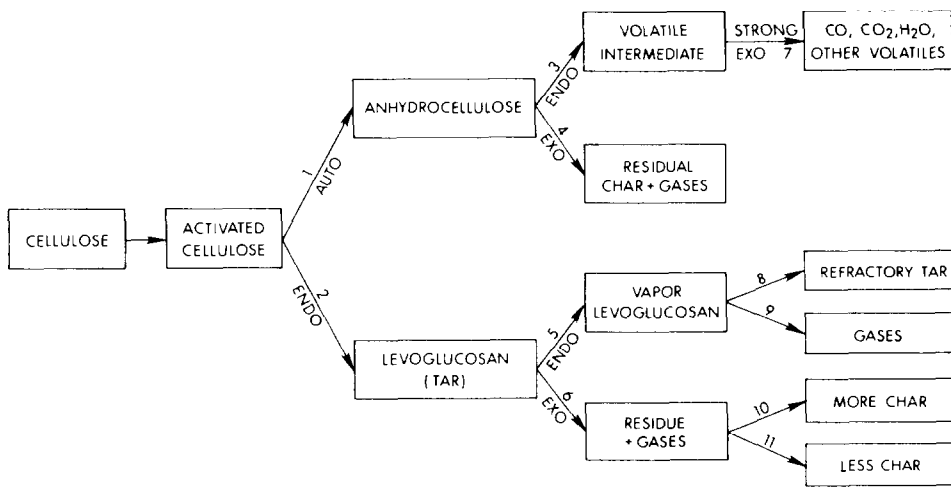

Fig. 17. A detailed mechanism for cellulose pyrolysis.

reaction 7 (Fig. 17). The exothermicity of this reaction, which normally lowers the total heat of pyrolysis, is absent. Before volatile traps were installed, a dramatic flow drop during pyrolysis under a high flow was observed. This flow drop indicated the presence of large uncracked volatile molecules existing through the fine valves, hence supporting the above explanation. At the same time, ΔH_{pyr} is higher because high flows favor endothermic vaporization of levoglucosan (reaction 5) over exothermic decomposition (reaction 6).

Our results also show a smaller char yield at high flows; while with a low flow, the char yields are higher but more scattered. Here, two types of char must be distinguished. Visually, the primary char has a strong structural integrity, retaining the shape of the original sample. The formation of this residual char is thus a solid phase phenomenon, apparently through the reactions 1 and 4 sequence. The secondary char is soft and fluffy, resembling the char from pyrolysis of levoglucosan, and is presumed to be the product of reaction 6. Char yields are higher with a low flow because these conditions correspond to a mass transfer limiting situation for the escape of levoglucosan, conditions which favor reaction 6 over 5. Since secondary char is formed from volatiles in a liquid or gaseous state, it does not remain inside the sample boat. The difficulty in collecting and accurately measuring the amount of secondary char leads to the scattering of low flow char yields.

The reasons for pressure favoring char formation in cellulose pyrolysis follow immediately from the proposed mechanism. The previous sections conclude that pressure favors reaction 4 over 3, and 6 over 5. Both reactions 4 and 6 result in char formation.

Pressure can affect the total heat of pyrolysis in two major opposing ways. First, it favors the exothermic reaction 6 over the endothermic reaction 5, thus lowering the total heat of pyrolysis. This is also evidenced by the

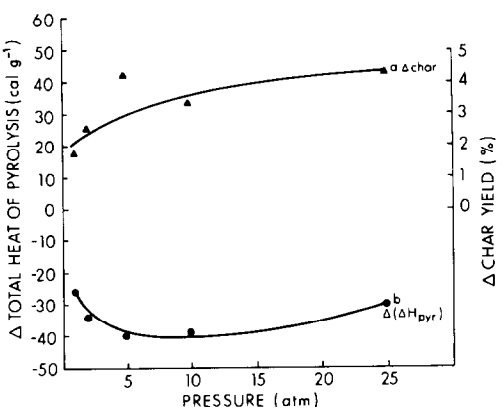

Fig. 18. Plot of differences in the heat of pyrolysis [●, ΔH_{pyr}(low) − ΔH_{pyr}(high)] and in char yields [▲, char(low) − char(high)] vs. pressure.

dramatic increase in endothermicity under vacuum, when almost all the levoglucosan is volatilized instead of decomposed. Secondly, high pressure favors the exothermic reaction 4 over reaction 3. However, under a low flow, reaction 3 actually leads to the more exothermic formation of permanent gases (reaction 7). The increased role of reaction 4 diminishes the exothermic effect of reaction 7, and thus causes the overall heat of pyrolysis to increase. The fact that the overall result indicates a decrease of ΔH_{pyr} with increasing pressure suggests the former to be the dominant effect.

Having understood the basic effects of flow rate and pressure independently, it is of interest to examine how the two effects interact with each other. At any constant pressure, the difference between char yields from pyrolysis with different flow rates [(Δchar = char(low flow) − char(high flow)] is effected by the additional activity of reaction 6 under a low flow. However, the difference in the heat of pyrolysis [$\Delta\Delta H_{pyr} = \Delta H_{pyr}$(low flow) − ΔH_{pyr}(high flow)] is brought about both by the additional activity of reaction 6 and by the additional exothermicity from reaction 7. Plotting these differences (which represent the effect of flow rates) against pressure (Fig. 18) furnishes further support for the present mechanism. Increasing Δchar with pressure implies that the amount of increased activity of reaction 6 due to a low flow increases with pressure. This is in agreement with the initial part of curve b of Fig. 18, which shows that the additional exothermicity caused by low flow also increases with pressure. However, this curve continues on to show a reverse effect. Such phenomenon can be easily explained by the present mechanism. With increasing pressure, less volatile intermediate and less vapor phase levoglucosan are formed. Consequently, there are less volatiles available to react by the exothermic reaction 7. This aspect of the mechanism dictates then, with increasing pressure, a diminishing effect of low flow in favoring exothermicity. This effect overrides the earlier effect and gives rise to a minimum in the curve.

The only remaining question is how pressure affects the primary competition between reactions 1 and 2. It is known that dehydration to form anhydrocellulose is the dominant reaction at the preheating temperature of 240°C, and that the extent of the reaction, accompanied by the evolution of H_2O, can be measured by weight loss. To study the effect of pressure on the primary pair of competitive reactions, cellulose samples were heated at

TABLE 6

Weight loss after preheating cellulose at 240°C for 2 h (%)

Pressure (atm)	Flow	
	Low	High
1	5	6
25	6	4

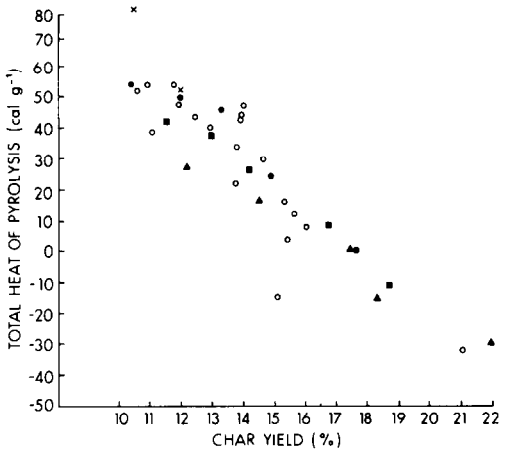

Fig. 19. Plot of heat of pyrolysis of cellulose vs. char yield.

240°C for 2 h and weight loss after preheating was measured. Experiments were conducted at 1 and 25 atm at low and high flows, and the results are shown in Table 6. No significant difference in weight loss is evident. These results suggest that equal amounts of anhydrocellulose are formed during preheating at both pressures, implying that pressure has no effect on the primary competitive reactions. Since only solid phase reactions are involved, the null effect might have been expected. The experimental results also indicate that flow rate exerts no effect on the primary solid phase reactions, justifying our assumption that flow rate influences cellulose pyrolysis only through secondary vapor phase reactions.

Finally, an interesting observation can be made by plotting the total heats of pyrolysis vs. char yields (Fig. 19). Clearly, reactions are more exothermic with higher char yields. However, there is no reason to believe that the relationship between char yield and heat of pyrolysis should be linear, since more than one reaction controls char formation. The fact that the data cluster along a straight line suggests either that all char formation reactions have about the same heat of reaction, or that one type of char is particularly dominant. Earlier, it was assumed that primary char is the dominant char form. This result seems to support the assumption.

CONCLUSIONS

The use of a high pressure micro reactor system in conjunction with a differential scanning calorimeter to study biomass pyrolysis has proven successful, not only in providing engineering data concerning the heat demands of pyrolysis, but also in furnishing mechanistic information. While the DSC data evidence only one peak representing the entire pyrolysis

process, carefully planned experiments permit not only the extraction of general information about the overall process, but specific details regarding the individual reactions involved in the complex degradation scheme.

To summarize, the following contributions have been made by this study:

(1) this is the first systematic study regarding pressure effects on the heat demand of cellulose pyrolysis;

(2) heat of pyrolysis data have been obtained over a range of experimental conditions, suitable for engineering applications, particularly in reactor designs;

(3) pressure is found to favor char formation and decrease the total heat of pyrolysis;

(4) the flow of purge gas, or the residence time of volatiles in the hot reactor, determines the extent of exothermic secondary volatile reactions. High flow also promotes evaporation of levoglucosan, and minimizes 'secondary' char formation. Overall, a high flow leads to lower char yields and higher total ΔH_{pyr};

(5) it is observed that very similar sets of competitive reactions leading to char or volatiles seem to govern the degradation process of all intermediate compounds involved in cellulose pyrolysis;

(6) an expanded mechanism describing cellulose pyrolysis has been postulated. This mechanism explains the various observed effects of pressure and flow rate.

The expanded mechanism of cellulose pyrolysis postulated here leaves much room for further experimental verification. Although phase 1 of this research has explored the effects of pressure on the product distribution, that work incorporated severe gas phase cracking into the pyrolysis process. An experimental setup (which allows tar collection and liquid analysis) to study the effects of pressure and flow rate on the product distribution under conditions similar to the present work could be used to critically evaluate the present mechanism.

The entire discussion of the anhydrocellulose pyrolysis mechanism has been based on the difference in results of pyrolysis with and without preheating. Experiments employing a large fraction of anhydrocellulose as a starting material, produced perhaps by a prolonged preheat treatment, are necessary to further characterize the reactions of anhydrocellulose.

Finally, uncertainty remains concerning the levoglucosan pyrolysis mechanism, particularly with regard to the residue reactions. By manipulating various parameters, such as pressure, flow rate and heating rate, one can cause the material to degrade by a particular route leading to where the uncertainties lie, and then conduct further investigations.

ACKNOWLEDGEMENTS

The authors wish to express their thanks to Drs. T. Reed and T. Milne (SERI), D. Stevens (BPNL) and S. Frederick and B. Berger (USDOE) for

their interest in this work. The technical assistance of Mr. William E. Edwards was appreciated. This work was supported by the Battelle Pacific Northwest Laboratories under subcontract No. B-C5822-A-Q.

REFERENCES

1 W.S.-L. Mok and M.J. Antal, Thermochim Acta, 68 (1983) 155.
2 F. Kilzer and A. Broido, Pyrodynamics, 2 (1965) 151.
3 D. Arseneau, Can. J. Chem., 49 (1971) 632.
4 A. Bradbury, Y. Sakai and F. Shafizadeh, J. Appl. Polym. Sci., 23 (1979) 3271.
5 T. Gluick, Senior Thesis, Chemistry Dept., Princeton University, 1980.
6 M. Ramiah, J. Appl. Polym. Sci., 14 (1970) 1323.
7 A. Roberts, J. Appl. Polym. Sci., 14 (1970) 244.
8 A. Lipska and W. Parker, J. Appl. Polym. Sci., 13 (1969) 851.
9 W. Mok, MSE Thesis, Princeton University, 1982.
10 F. Shafizadeh, G. McGinnis, R. Sucott and C. Philpot, Carbohydr. Res., 15 (1970) 165.
11 W.S.-L. Mok and M.J. Antal, Proc. 13th Biomass Thermochemical Conversion Contractor's Meeting, CONF-8110115, PNL-SA-10039, (1981), p. 399.
12 A. Broido, M. Evett and C. Hodges, Carbohydr. Res., 44 (1975) 267.
13 H.L. Friedman, J. Polym. Sci., Part C, 6 (1964) 183.
14 M.J. Antal, in B. Miller (Ed.), Thermal Analysis: Proceedings of 7th ICTA, Wiley, New York, 1982, p. 1490.
15 M.J. Antal, Ind. Eng. Chem. Prod. Res. Dev., 22 (1983) 366.
16 J.H. Flynn, Thermochim. Acta, 37 (1980) 225.
17 M. Cerny and F. Stanek, Fortschr. Chem. Forsch., 14 (1970) 526.